Authors:
Sylvain Carbes (SC)

Aalborg, 2011.04.28

Shoulder Rhythm

Contents:

AnyBody Technology A/S · Niels Jernes Vej 10 · DK-9220 Aalborg East · Denmark · Phone +45 9635 4286 · Fax +45 9635 4599
www.anybodytech.com · anybody@anybodytech.com · CVR no. 26367042

1 Summary

In order to improve the shoulder model of the AnyBody Modeling System a shoulder rhythm has been developed, defining the motion of the scapula and the clavicle as a function of humerus motion. The shoulder rhythm has been implemented with the data from JH de Groot, R Brand [1]. The paper provides 5 linear equations describing the rotation of the clavicle and scapula regarding to the thorax as a function of the humerus elevation and flexion. The equations describe the rotations corresponding to clavicle protraction, clavicle elevation, scapula protraction, scapula elevation and scapula tilt.
The aim of the shoulder rhythm is to provide a more realistic model of the shoulder that plays an important role in many applications.

2 Implementing of the shoulder rhythm

2.1 Description of the old joint

The AnyBody shoulder model is based on the Dutch Shoulder Group model. The structure of the shoulder articulation is the following:

- Clavicle is attached to the thorax by a spherical joint + 3 rotational drivers.
- Scapula is attached to the clavicle by a spherical joint + 2 sliding points on the rib cage wich is modelled as an ellipsoid and the conoid ligament between scapula and clavicle (constant distance).
- Humerus is attached to the scapula by a spherical joint + 3 rotational drivers.

See Figure 1.
For most applications the clavicle and scapula has until now been in a fixed neutral position.

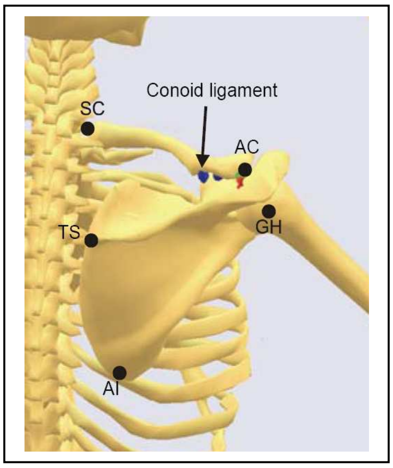

- SC Spherical joint
- AC Spherical joint
- GH Spherical joint
- TS Scapula thoracic gliding plane, ellipsoid
- AI Scapula thoracic gliding plane, ellipsoid
- Conoid ligament, constant length

Figure 1: Structure of the shoulder Girdle.

The local reference frame is represented for each segment on Figure 2.

AnyBody Technology A/S · Niels Jernes Vej 10 · DK-9220 Aalborg East · Denmark · Phone +45 9635 4286 · Fax +45 9635 4599
www.anybodytech.com · anybody@anybodytech.com · CVR no. 26367042

ANYBODY TECHNOLOGY

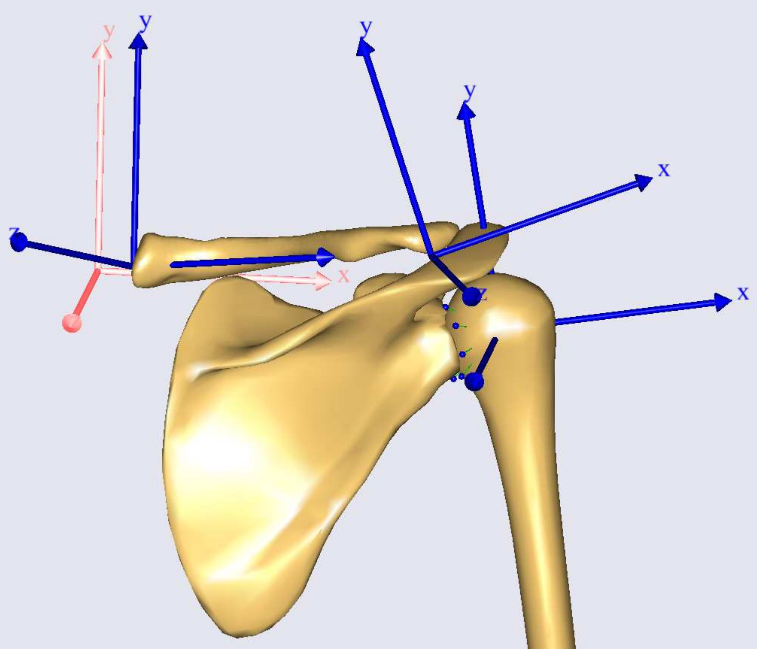

Figure 2: Local Coordinate systems of the elements of the shoulder (in blue the Humerus, Scapula, Clavicle and in red the Thorax reference node).

2.2 Implementation of the kinematics with equations of motion

Based on the paper of JH de Groot, R Brand [1] six equations have been implemented to drive the rotation of the clavicle and scapula regarding to the thorax. Table 3 of the paper gives the coefficients and constants of the linear regression from measured orientation of both bones. The table only gives the linear regression parameters for clavicle protraction, clavicle elevation, scapula protraction, scapula elevation and scapula tilt (all motions are calculated in a specially oriented thorax reference frame; called ShoulderRef in our model). They are function of humerus elevation, humerus flexion, force applied and initial position. The parameters for clavicle axial rotation are not present, so the equation had to be extrapolated directly from a graph of JH de Groot [2]. The graph shows the measured axial rotation of the clavicle regarding to the thorax during arm elevation, Figure 3.
In the table the linear regression equations are function of the following parameters:

- Cy: clavicle protraction
- Cz: clavicle elevation
- Sy: scapula protraction
- Sz: scapula elevation
- Sx: scapula tilt
- C: constant
- Hy: humerus flexion
- Hz: humerus elevation
- F: force applied (not taken into account in our model)
- Xo: initial position

The resulting equations are of the following form (example with Cy):

AnyBody Technology A/S · Niels Jernes Vej 10 · DK-9220 Aalborg East · Denmark · Phone +45 9635 4286 · Fax +45 9635 4599
www.anybodytech.com · anybody@anybodytech.com · CVR no. 26367042

$$Cy = -0{,}242 * Hz + 0{,}12 * Hy + 0{,}851 * (-0{,}401) - 4{,}983 * pi/180$$

Clavicle protraction (Rad)

Coefficient for Hz from the table

Coefficient for Hy from the table

Coefficient for Xo from the table

Xo: initial position of the bone in AnyBody (Rad)

Constant from the table (given in Deg)

Applying those coefficients to the initial position of our model, we get the following equations:

$$Cy = -0{,}242 * Hz + 0{,}12 * Hy + 0{,}851 * (-0{,}401) - 4{,}983 * pi/180$$

$$Cz = 0{,}123 * Hz - 0{,}046 * Hy + 0{,}493 * 0{,}201 + 3{,}917 * pi/180$$

$$Sy = -0{,}049 * Hz + 0{,}14 * Hy + 0{,}901 * 0{,}33 - 1{,}203 * pi/180$$

$$Sz = 0{,}396 * Hz - 0{,}079 * Hy + 0{,}414 * 0{,}307 + 3{,}095 * pi/180$$

$$Sx = 0{,}184 * Hz - 0{,}028 * Hy + 0{,}886 * (-0{,}101) + 0{,}659 * pi/180$$

Those equations apply to the right arm, they have been mirrored to fit the left arm.

As mentioned previously, there is no linear regression for the clavicle axial rotation in the paper of JH de Groot, R Brand [1]. So this equation has been extrapolated manually from the graph of the phd report from JH de Groot [2], Figure 3 and Figure 4. This graph displays the axial rotation of the clavicle as function of the humerus elevation only. Humerus flexion is so far no taken into account in the clavicle axial rotation equation. Due to the lack of information, the appropriate constant for this equation has been found iteratively so that the orientation of the clavicle in neutral position is exactly the same as it is without the rhythm. The equation results to be the following:

$$Cx = 0{,}422 * Hz - 0{,}423$$

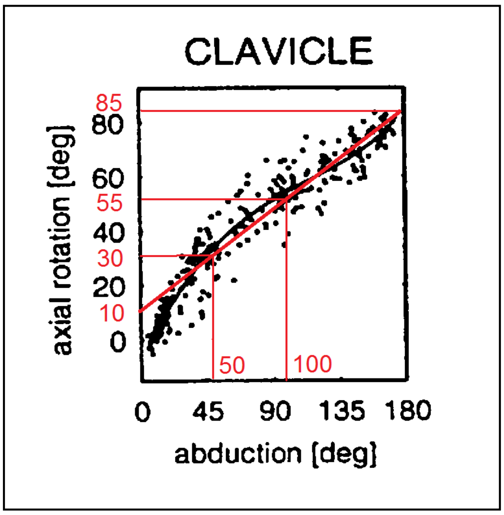

Figure 3: Recorded clavicle axial rotation during humerus elevation (reprinted from JH de Groot [2]). The red line represents the linear regression of the curve extrapolated manually and then calculated in Figure 4.

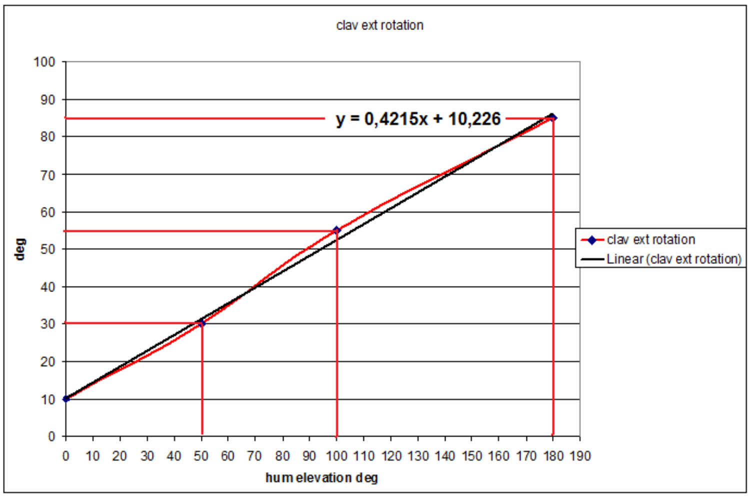

Figure 4: Linear regression for the clavicle axial rotation.

In order to add those 6 equations driving 6 dof in the model, we removed the corresponding drivers on the previous model: the 3 rotational drivers for the SC joint, the two sliding constraints of the scapula on the rib cage and the fixed length of the conoid ligament.

2.3 Kinematic validation

After the first visual check on the model view to verify if the new motion is correct, several graphs have been plotted from the AnyBody model to be compared with the graphs of JH de Groot, R Brand [1] (Figure 3 of the paper). De Groot's graphs show point clouds of the recorded positions, so to compare with the AnyBody curves a linear regression has been manually extracted from the point cloud. All the graphs are matching in terms of coefficient, however almost each AnyBody curve present an offset value compared to the corresponding curve from JH de Groot, R Brand [1], Figure 5, 6, 7, 8 and 9. This offset is explained by the difference of initial positions between the AnyBody model and the experiment's subject. However scapula and clavicle's initial position of the AnyBody model are known to miss accuracy. So the choice has been made to use the experiment's subject initial position in the AnyBody model by subtracting the constant corresponding to the offset in the drivers equations.

AnyBody Technology A/S · Niels Jernes Vej 10 · DK-9220 Aalborg East · Denmark · Phone +45 9635 4286 · Fax +45 9635 4599
www.anybodytech.com · anybody@anybodytech.com · CVR no. 26367042

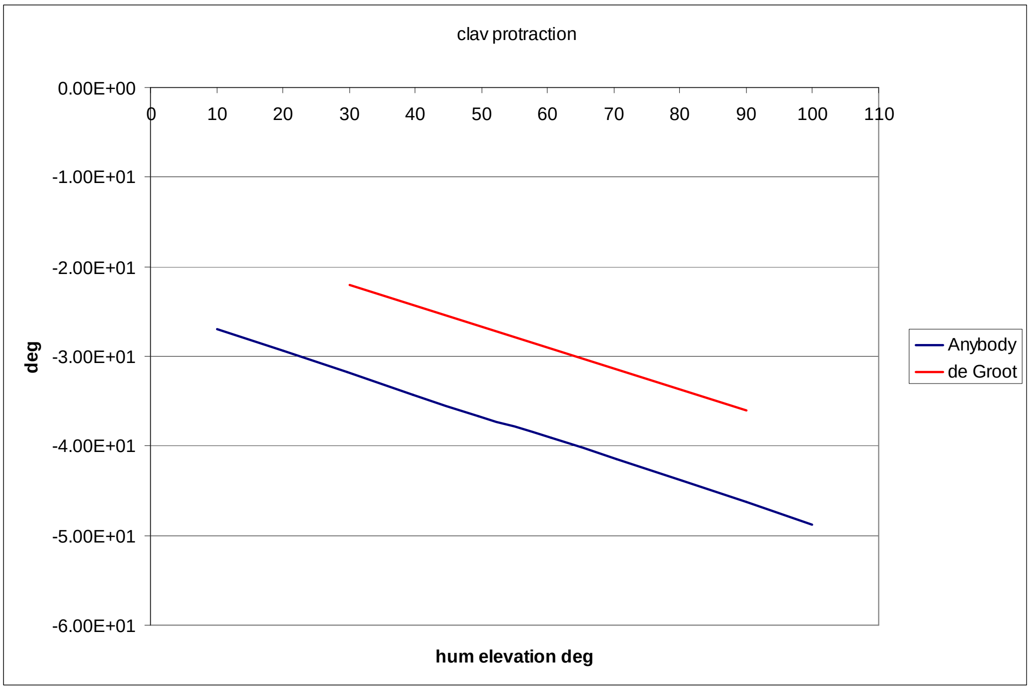

Figure 5: Clavicle protraction recorded by de Groot (red) and predicted from AnyBody(blue).

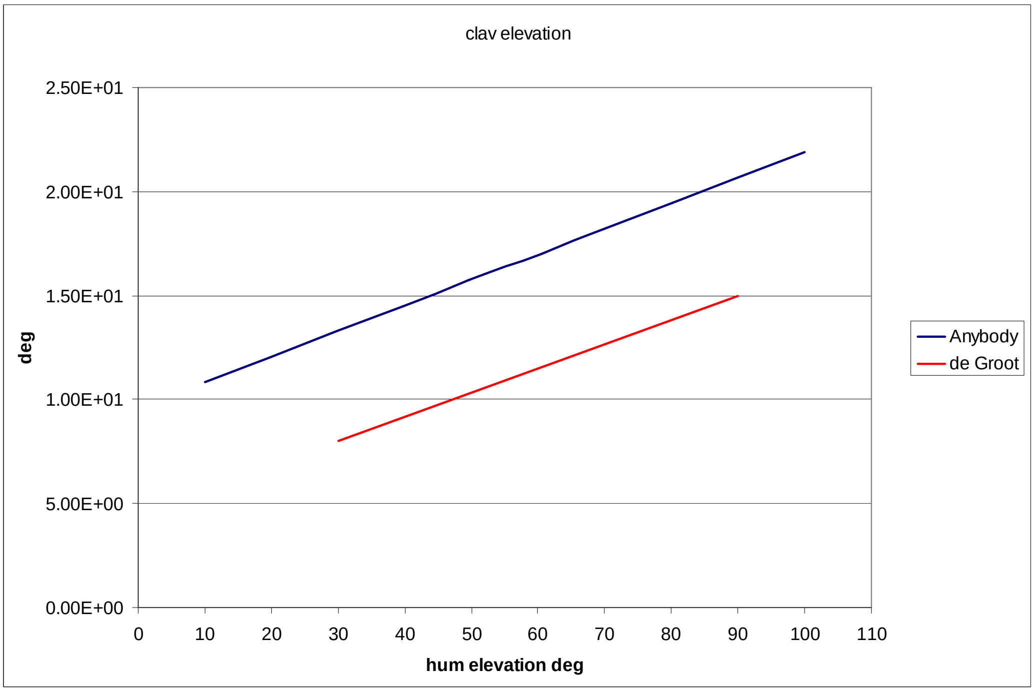

Figure 6: Clavicle elevation recorded by de Groot (red) and predicted from AnyBody(blue).

AnyBody Technology A/S · Niels Jernes Vej 10 · DK-9220 Aalborg East · Denmark · Phone +45 9635 4286 · Fax +45 9635 4599
www.anybodytech.com · anybody@anybodytech.com · CVR no. 26367042

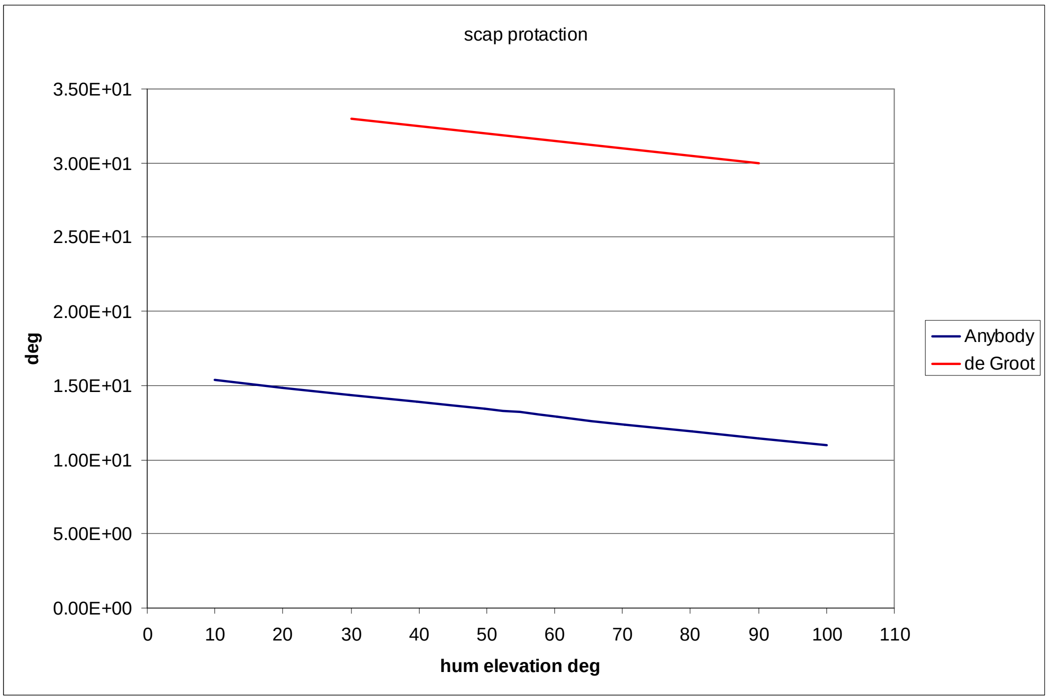

Figure 7: Scapula protraction recorded by de Groot (red) and predicted from AnyBody(blue).

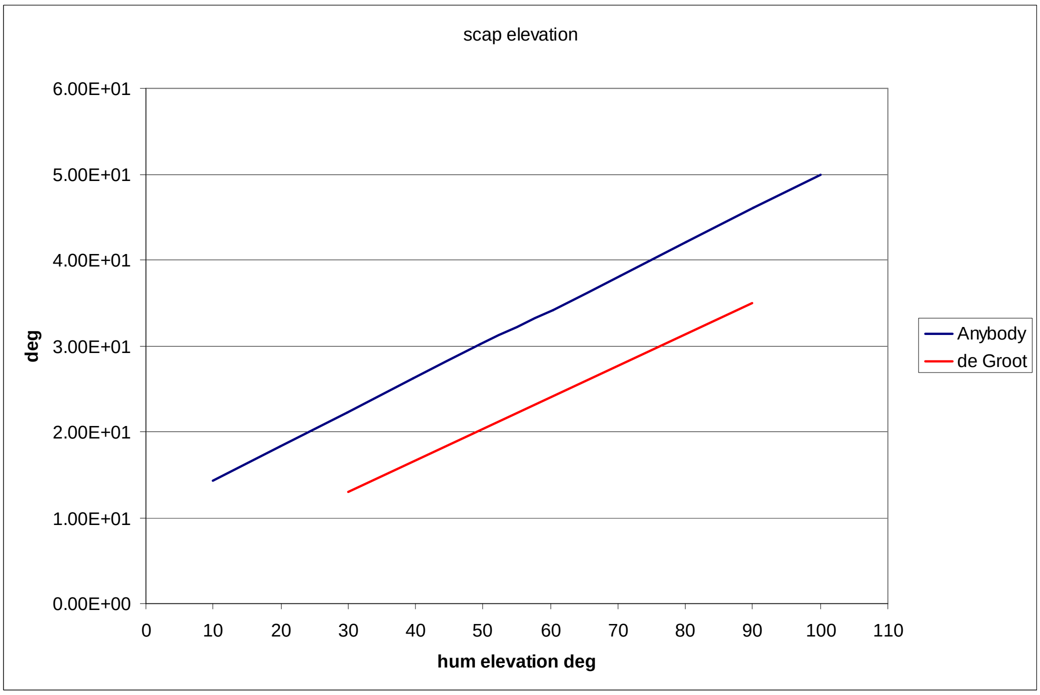

Figure 8: Scapula elevation recorded by de Groot (red) and predicted from AnyBody(blue).

AnyBody Technology A/S · Niels Jernes Vej 10 · DK-9220 Aalborg East · Denmark · Phone +45 9635 4286 · Fax +45 9635 4599
www.anybodytech.com · anybody@anybodytech.com · CVR no. 26367042

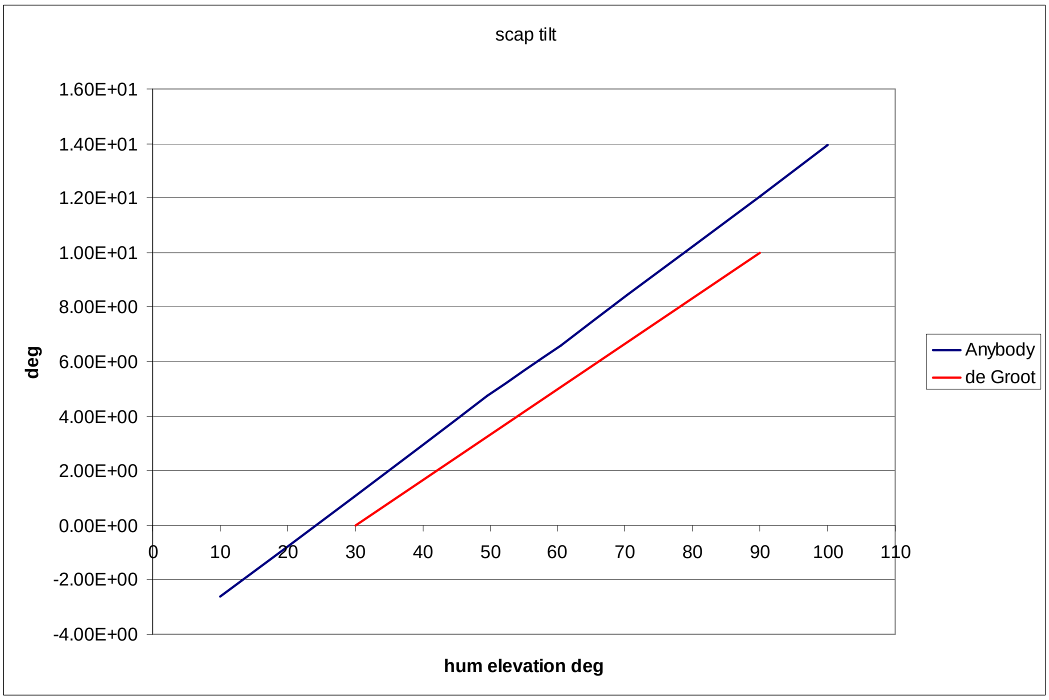

Figure 9: Scapula tilt recorded by de Groot (red) and predicted from AnyBody(blue).

If we look at the kinematic measure, we can see that the AI point stay very close to the ellipsoid representing the rib cage, from 6,6 mm to 0,7 mm of distance, Figure 10.

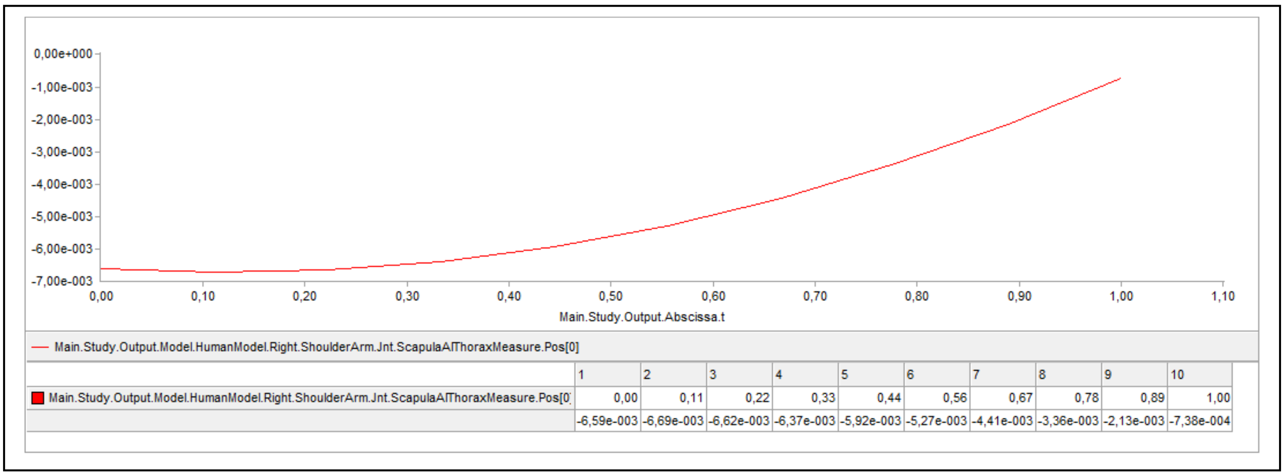

Figure 10: Distance from the scapular AI point to the ellipsoid of the rib cage during scapula motion.

2.4 Boundary conditions

As seen previously, the trajectory of the AI point is very close to the old one sliding along the rib cage, Figure 10. So the choice has been made to include the AI sliding constraint again. The corresponding scapula tilt constraint is then removed to maintain dof balance.

AnyBody Technology A/S · Niels Jernes Vej 10 · DK-9220 Aalborg East · Denmark · Phone +45 9635 4286 · Fax +45 9635 4599
www.anybodytech.com · anybody@anybodytech.com · CVR no. 26367042

The aim of switching back to the sliding constraint is to allow us to use the unilateral reaction force due to the contact between the scapula and the rib cage. This way we can provide realistic boundary conditions to the scapula.

2.5 Force validation

In order to validate the model in terms of forces we tested it in three different applications:

- BergmannGH, already used to validated the previous shoulder model.
- GrootEMG, based on an experiment from JH de Groot, LA Rozendaal, CGM Meskers, HJ Arwert [3], compare activation with measured EMG data.
- PushUp, simulation of a person doing push up.

2.5.1 BergmannGH

This model is based on the experiment of Bergmann et al [4] measuring in vivo reaction forces in the glenohumeral joint during arm abduction. A maximum of 880 Newtons has been recorded in the experiment. The measurement results can be seen at www.orthoload.com. This model has been used previously to validate the shoulder model without Rhythm. The results obtained with the model without rhythm showed that the model is behaving similarly to the human shoulder. However the magnitude of the reaction forces was lower in the model than in the experiment, this is because of uncertainties due to the non scaled model (no information available about segment's length and mass), Figure 11.

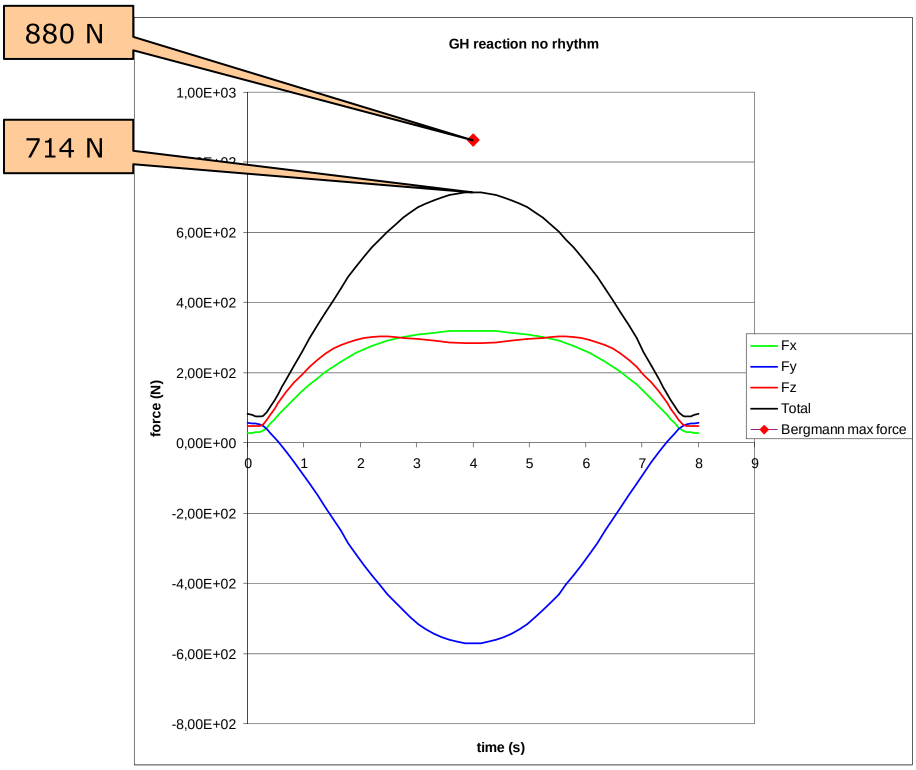

Figure 11: Forces on GH joint calculated from AnyBody for the shoulder model without rhythm.

AnyBody Technology A/S · Niels Jernes Vej 10 · DK-9220 Aalborg East · Denmark · Phone +45 9635 4286 · Fax +45 9635 4599
www.anybodytech.com · anybody@anybodytech.com · CVR no. 26367042

The results of the model with the shoulder rhythm are quite similar to the previous ones, Figure 12. However some differences have to be noticed. First, the maximum of the total reaction force is higher when using the shoulder rhythm. It becomes closer to the 880 N from Bergmann et al [4] by reaching 758 N instead of 714 previously.
Then the behaviour of Fx and Fz is also interesting. In the experiment Fx curve is closely following Fz curve with Fx superior to Fz. The model without rhythm was not recreating this behaviour very well, it can be seen in the Figure 11 that at the beginning Fz is higher than Fx, then becomes lower than Fx at the maximum abduction and switch back again to be higher at the end of the movement.
The rhythm model reproduces much better the behaviour of Fx and Fz: like in the experiment Fx is a sensitively higher than Fz.
Both models are still very close, despite those improvements the general behaviour of the shoulder that was previously validated remains the same, Figure 13.

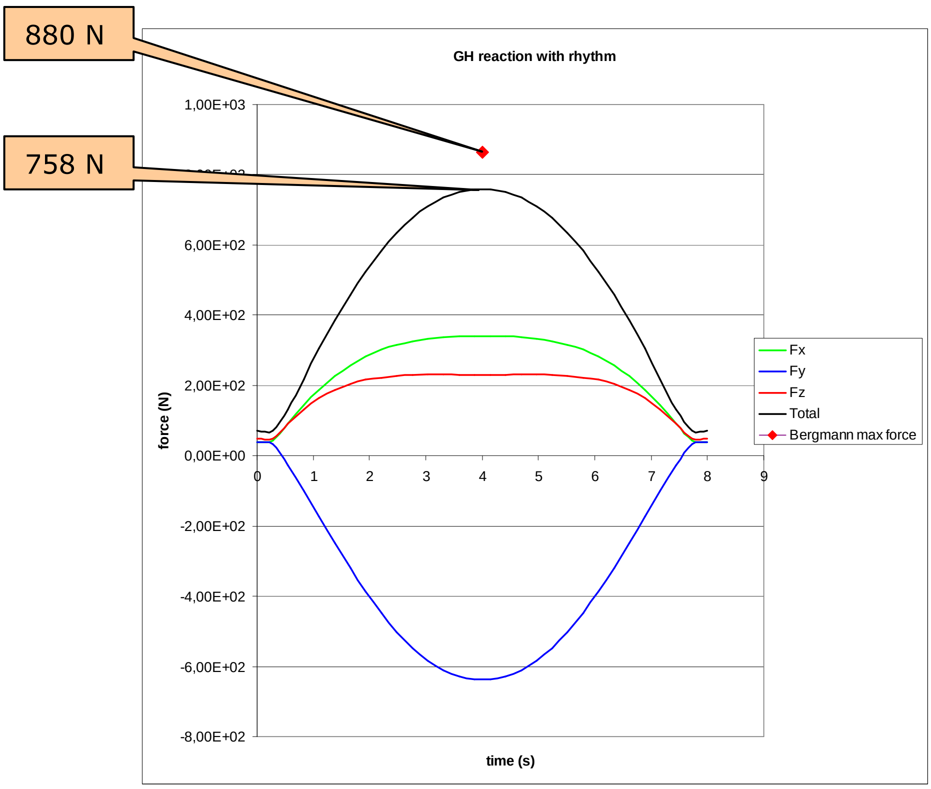

Figure 12: Forces on GH joint calculated from AnyBody for the new shoulder rhythm model.

AnyBody Technology A/S · Niels Jernes Vej 10 · DK-9220 Aalborg East · Denmark · Phone +45 9635 4286 · Fax +45 9635 4599
www.anybodytech.com · anybody@anybodytech.com · CVR no. 26367042

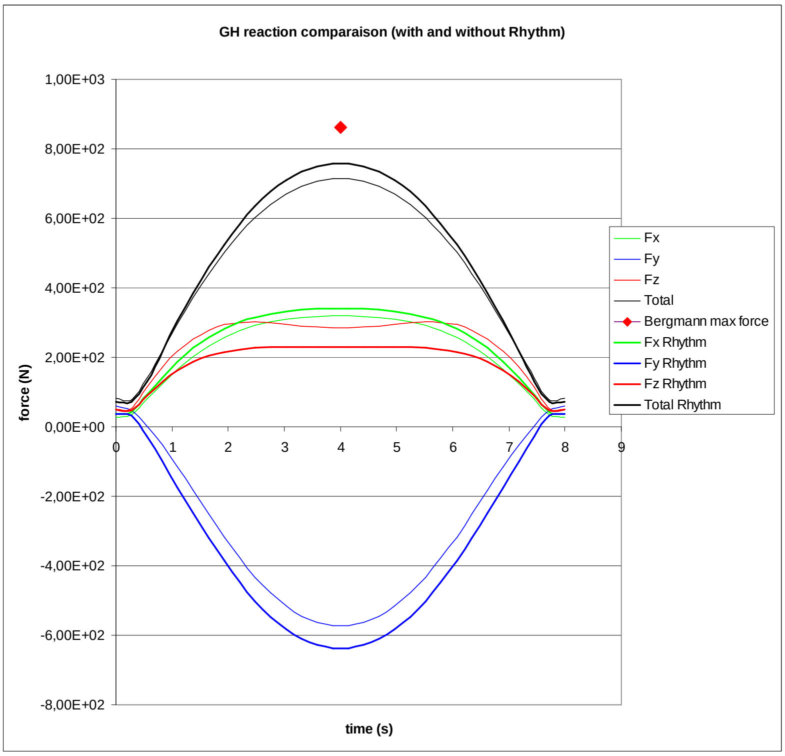

Figure 13: Comparison of forces on GH joint calculated from AnyBody for the shoulder model with and without rhythm.

2.5.2 GrootEMG

This application reproduces an experiment from JH de Groot, LA Rozendaal, CGM Meskers, HJ Arwert [3]. In the experiment the EMG of 12 muscles of the shoulder have been recorded for a force applied to the arm in 20 different directions (from 0° to 360°). The results can be seen as graphs showing muscle EMG function of the angle of application of the force.
In the graphs from JH de Groot [3] the dots represent the measured EMG and the line represent estimated EMG from a shoulder model developed by JH de Groot [3].
The experiment has been reproduced in AnyBody and the muscle activation graphs have been compared to the corresponding EMG graphs from JH de Groot [3], Figure 14 to 23.

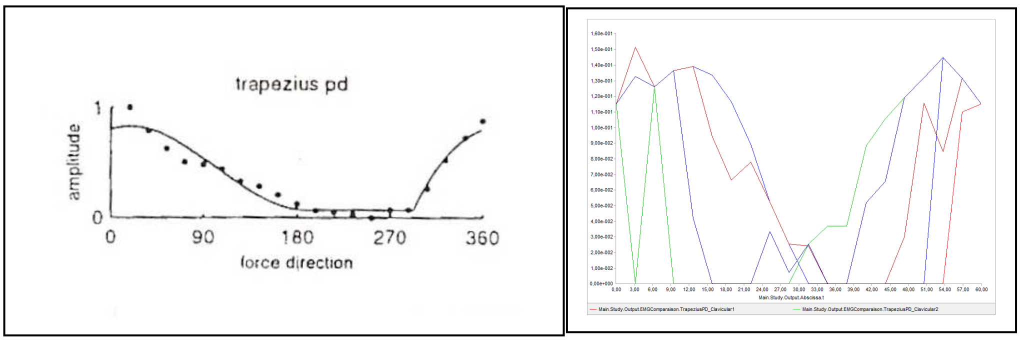

Figure 14: Recorded EMG (reprinted from JH de Groot [3]) and muscle max activity from AnyBody, trapezius clavicular.

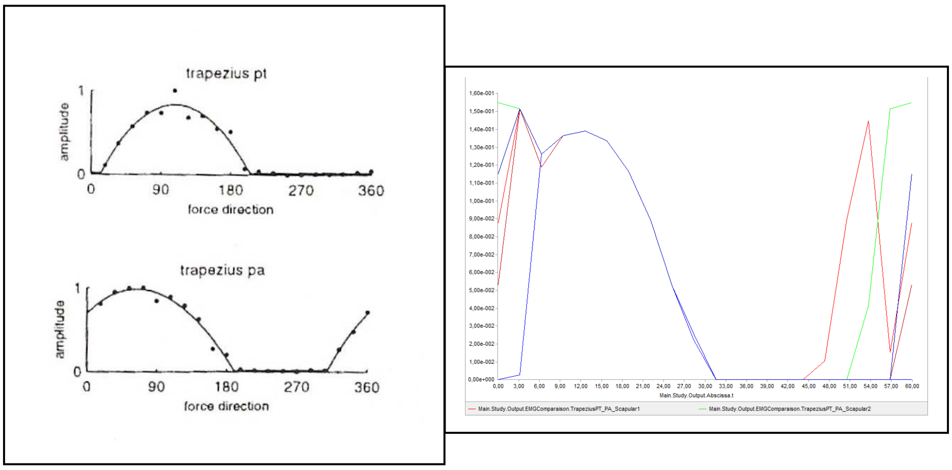

Figure 15: Recorded EMG (reprinted from JH de Groot [3]) and muscle max activity from AnyBody, trapezius scapular.

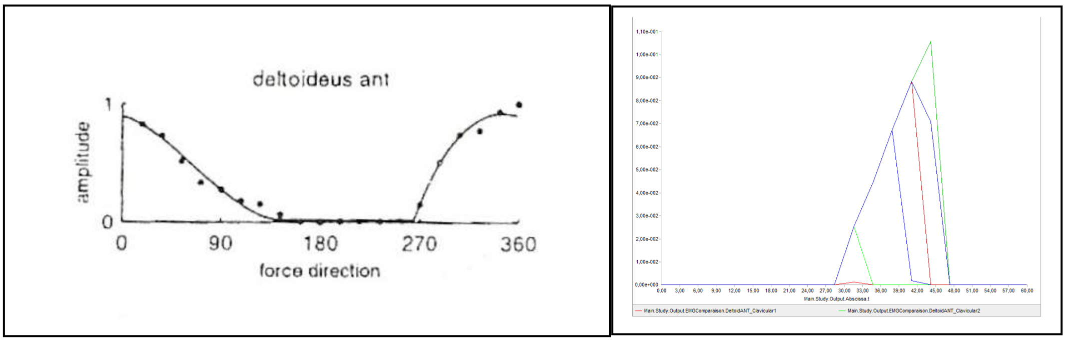

Figure 16: Recorded EMG (reprinted from JH de Groot [3]) and muscle max activity from AnyBody, deltoid clavicular.

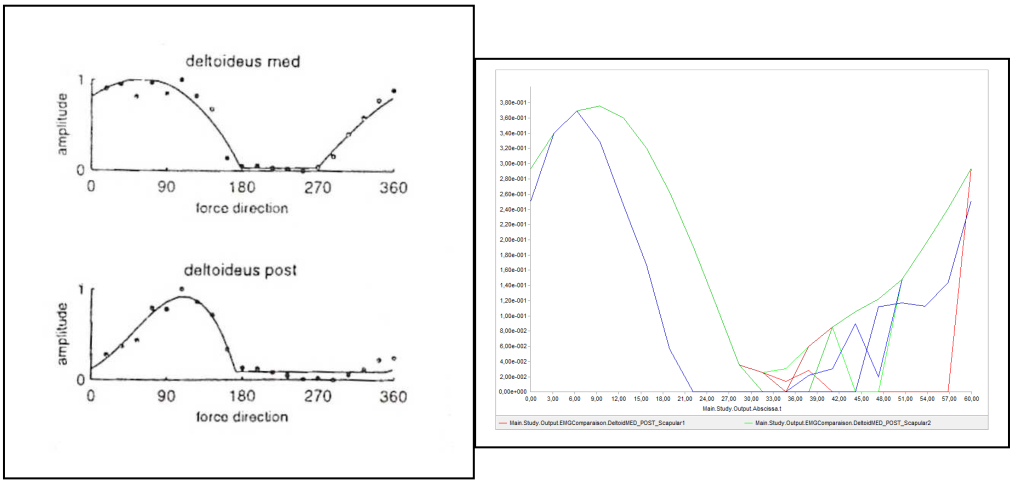

Figure 17: Recorded EMG (reprinted from JH de Groot [3]) and muscle max activity from AnyBody, deltoid scapular.

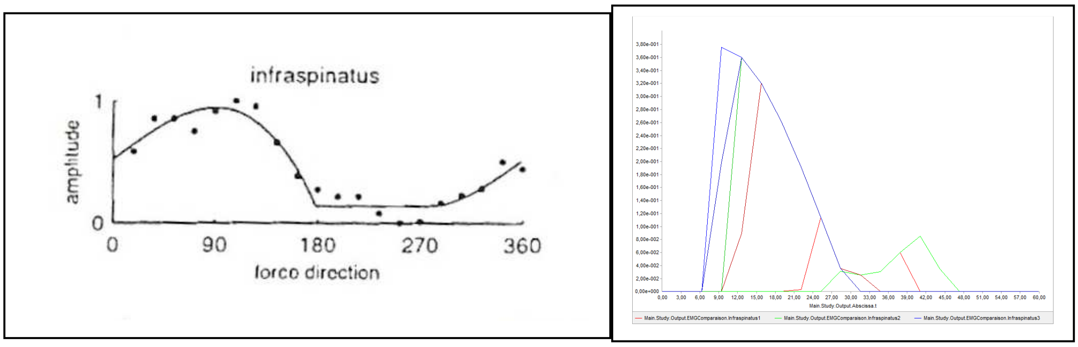

Figure 18: Recorded EMG (reprinted from JH de Groot [3]) and muscle max activity from AnyBody, infraspinatus.

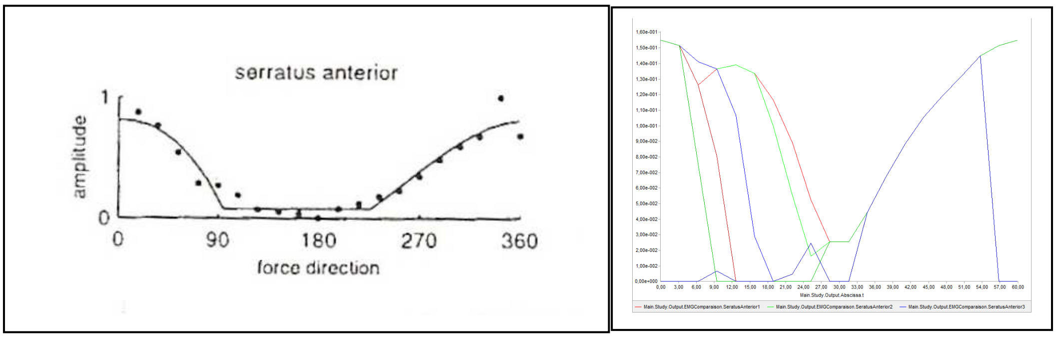

Figure 19: Recorded EMG (reprinted from JH de Groot [3]) and muscle max activity from AnyBody, serratus anterior.

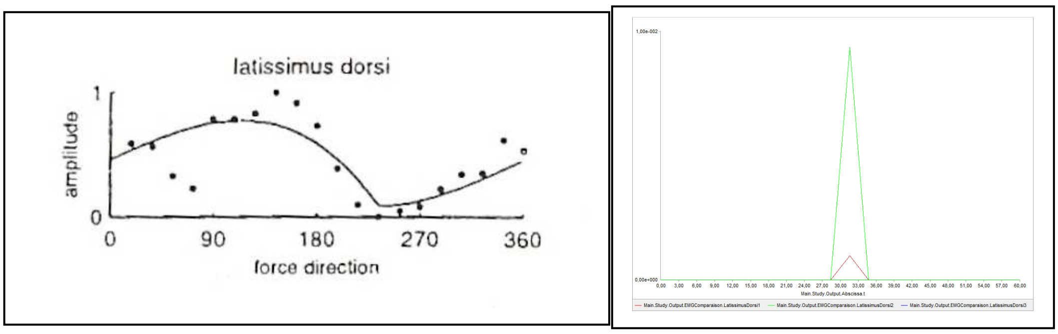

Figure 20: Recorded EMG (reprinted from JH de Groot [3]) and muscle max activity from AnyBody, latissimus dorsi.

AnyBody Technology A/S · Niels Jernes Vej 10 · DK-9220 Aalborg East · Denmark · Phone +45 9635 4286 · Fax +45 9635 4599
www.anybodytech.com · anybody@anybodytech.com · CVR no. 26367042

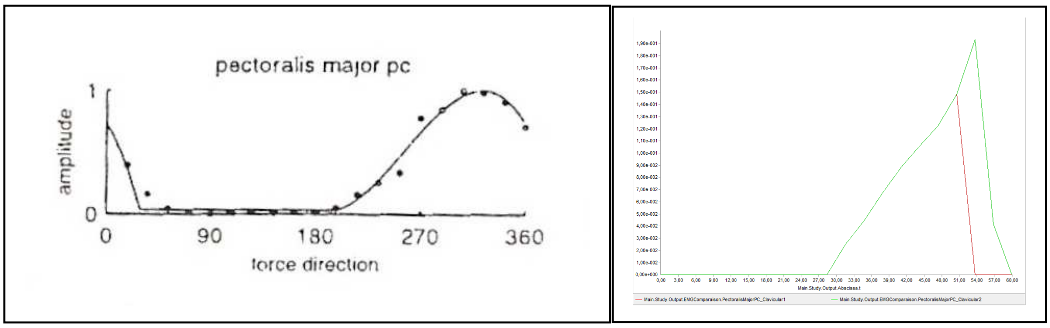

Figure 21: Recorded EMG (reprinted from JH de Groot [3]) and muscle max activity from AnyBody, pectoralis major pc.

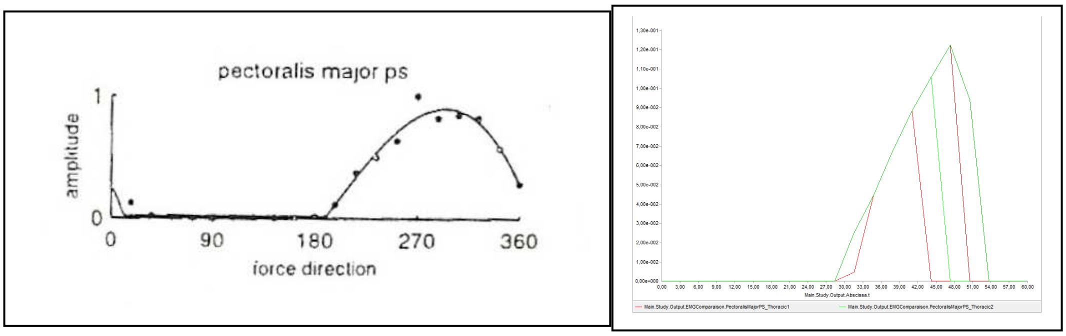

Figure 22: Recorded EMG (reprinted from JH de Groot [3]) and muscle max activity from AnyBody, pectoralis major ps.

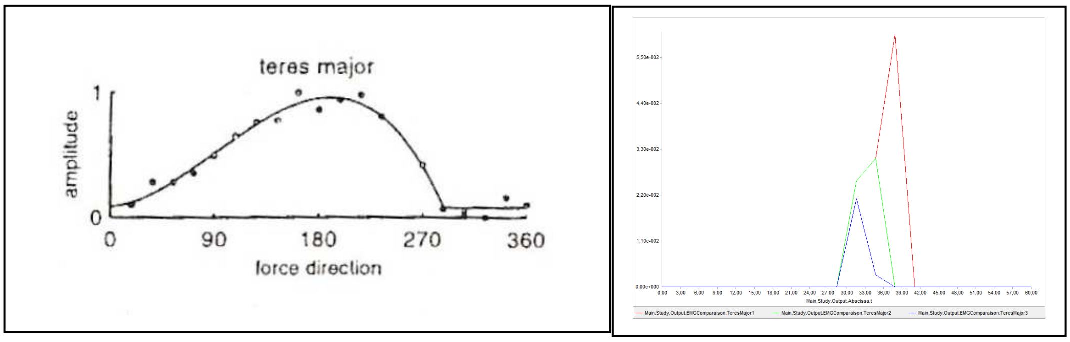

Figure 23: Recorded EMG (reprinted from JH de Groot [3]) and muscle max activity from AnyBody, teres major.

Except some differences for the deltoideus anterior, latissimus dorsi and the teres major, the recorded EMG and the muscle activation graphs are matching well. The shoulder rhythm model is considered as validated regarding to this experiment.

AnyBody Technology A/S · Niels Jernes Vej 10 · DK-9220 Aalborg East · Denmark · Phone +45 9635 4286 · Fax +45 9635 4599
www.anybodytech.com · anybody@anybodytech.com · CVR no. 26367042

2.5.3 PushUp

As a final test, the shoulder rhythm has been applied to the PushUp model. This model simulates a person doing push up.

The maximum muscle activity of the model with the shoulder rhythm is slightly higher than the one of the simple model (7% higher at the low position), Figure 24. The reaction force in the glenohumeral joint is a 15% higher with the shoulder rhythm during the low position of the push up movement, Figure 25. However the variation of the reaction force is much smoother with the shoulder rhythm, leading to less load jumps in the joint.

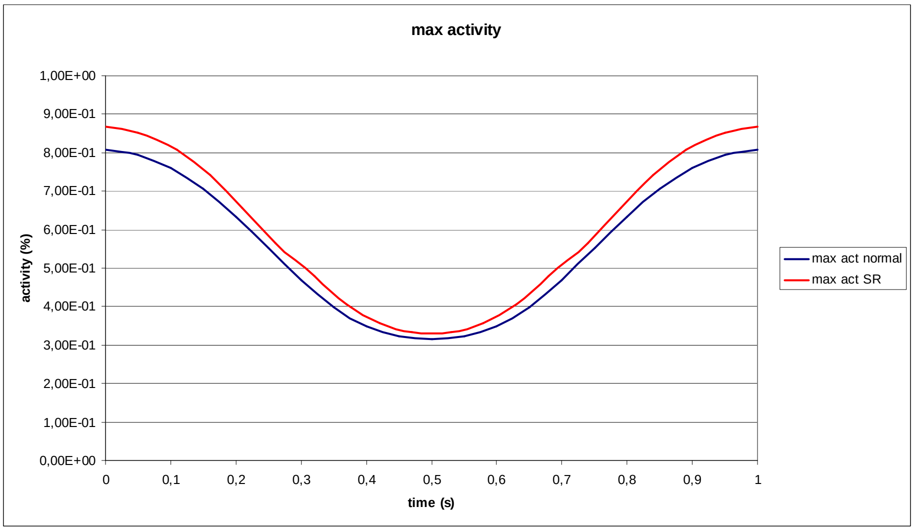

Figure 24: Comparison of maximum muscle activity for the simple model and the shoulder rhythm model.

Figure 25: Comparison of GH reaction force for the simple model and the shoulder rhythm model.

AnyBody Technology A/S · Niels Jernes Vej 10 · DK-9220 Aalborg East · Denmark · Phone +45 9635 4286 · Fax +45 9635 4599
www.anybodytech.com · anybody@anybodytech.com · CVR no. 26367042

3 Literature

[1] JH de Groot, R Brand. A three-dimensional regression model of the shoulder rhythm. Clin Biomech 2001;16:735-743.

[2] JH de Groot. The variance of the shoulder motions recorded by mean of palpation. Chapter 3, PHD report; The shoulder: a kinematic and dynamic analysis of motion and loading. 19/01/1998, University of Delft Germany. ISBN 90-9011298-7.

[3] JH de Groot, LA Rozendaal, CGM Meskers, HJ Arwert. Principal action of the EMG of the shoulder muscles during isometric loading in different directions. Chapter 8, PHD report; The shoulder: a kinematic and dynamic analysis of motion and loading. 19/01/1998, University of Delft Germany. ISBN 90-9011298-7.

[4] G Bergmann, F Graichen, A Bender, M Kääb, A Rohlmann, P Westerhoff. In vivo glenohumeral contact forces-Measurements in the first patient 7 months postoperatively. Journal of Biomechanics 2006;(vol40.issue10):2139-2149.

AnyBody Technology A/S · Niels Jernes Vej 10 · DK-9220 Aalborg East · Denmark · Phone +45 9635 4286 · Fax +45 9635 4599
www.anybodytech.com · anybody@anybodytech.com · CVR no. 26367042